Broadband wavelength conversion at 40 Gb/s using long serpentine As_2S_3 planar waveguides

Vahid G. Ta'eed[1], Mark D. Pelusi[1], and Benjamin J. Eggleton[1]
Duk-Yong Choi[2], Steve Madden[2], Douglas Bulla[2] and Barry Luther-Davies[2]

[1]*Centre for Ultrahigh-bandwidth Devices for Optical Systems (CUDOS), School of Physics, University of Sydney, NSW 2006, Australia*
[2]*Centre for Ultrahigh-bandwidth Devices for Optical Systems (CUDOS), Laser Physics Centre, The Australian National University, Canberra, ACT 0200, Australia*
vahid@physics.usyd.edu.au
http://www.physics.usyd.edu.au/cudos/

Abstract: We demonstrate broadband wavelength conversion of a 40 Gb/s return-to-zero signal by cross-phase modulation in a newly developed chalcogenide glass waveguide based photonic chip. These new serpentine As_2S_3 waveguides offer a nonlinear coefficient $\approx$1700 $W^{-1}km^{-1}$ with 5× lower propagation loss over a length of 22.5 cm which ensures the full propagation length contributes towards the nonlinear process. This reduces the peak operating power thereby allowing a ×4 increase in the data rate compared with previous results. Spectral measurements show the device operates over a span of 40 nm while system measurements show just over 1 dB of power penalty at a bit-error rate of 10^{-9}. This is primarily due to the compact planar waveguide design which minimizes the effect of group-velocity dispersion.

OCIS codes: (060.4510) Optical communications; (070.4340) Nonlinear optical signal processing; (190.2620) Frequency conversion; (130.3120) Integrated optics devices

References and links

1. B. Ramamurthy and B. Mukherjee, "Wavelength conversion in WDM networking," IEEE J. Sel. Areas Commun. **16**, 1061-1073 (1998).
2. G. P. Agrawal, *Nonlinear Fiber Optics* (Academic Press, San Diego, 2001).
3. J. Leuthold, L. Moller, J. Jaques, S. Cabot, L. Zhang, P. Bernasconi, M. Cappuzzo, L. Gomez, E. Laskowski, E. Chen, A. Wong-Foy, and A. Griffin, "160 Gbit/s SOA all-optical wavelength converter and assessment of its regenerative properties," Electron. Lett. **40**, 554-555 (2004).
4. B. E. Olsson, P. Ohlen, L. Rau, and D. J. Blumenthal, "A simple and robust 40-Gb/s wavelength converter using fiber cross-phase modulation and optical filtering," IEEE Photon. Technol. Lett. **12**, 846-848 (2000).
5. J. H. Lee, K. Kikuchi, T. Nagashima, T. Hasegawa, S. Ohara, and N. Sugimoto, "All-fiber 80-Gbit/s wavelength converter using 1-m-long Bismuth Oxide-based nonlinear optical fiber with a nonlinearity gamma of 1100 $W^{-1}km^{-1}$," Opt. Express **13**, 3144-3149 (2005).
6. V. G. Ta'eed, L. B. Fu, M. Pelusi, M. Rochette, I. C. M. Littler, D. J. Moss, and B. J. Eggleton, "Error free all optical wavelength conversion in highly nonlinear As-Se chalcogenide glass fiber," Opt. Express **14**, 10371-10376 (2006).
7. M. R. E. Lamont, V. G. Ta'eed, M. A. F. Roelens, D. J. Moss, B. J. Eggleton, D. Choy, S. Madden, and B. Luther-Davies, "Error-free wavelength conversion via cross phase modulation in 5 cm of As2S3 chalcogenide glass rib waveguide," Electron. Lett. **43**, 945-947 (2007).
8. M. Asobe, "Nonlinear optical properties of chalcogenide glass fibers and their application to all-optical switching," Opt. Fiber Technol. **3**, 142-148 (1997).
9. K. Yamada, H. Fukuda, T. Tsuchizawa, T. Watanabe, T. Shoji, and S. Itabashi, "All-optical efficient wavelength conversion using silicon photonic wire waveguide," IEEE Photon. Technol. Lett. **18**, 1046-1048 (2006).
10. E. M. Vogel, M. J. Weber, and D. M. Krol, "Nonlinear Optical Phenomena in Glass," Phys. Chem. Glasses **32**, 231-254 (1991).
11. V. Ta'eed, N. J. Baker, L. Fu, K. Finsterbusch, M. R. E. Lamont, D. J. Moss, H. C. Nguyen, B. J. Eggleton, D.-Y. Choi, S. Madden, and B. Luther-Davies, "Ultrafast all-optical chalcogenide glass photonic circuits," Opt. Express **15**, 9205-9221 (2007).

#87558 - $15.00 USD Received 14 Sep 2007; revised 24 Oct 2007; accepted 26 Oct 2007; published 30 Oct 2007

12. V. G. Ta'eed, M. Shokooh-Saremi, L. B. Fu, I. C. M. Littler, D. J. Moss, M. Rochette, B. J. Eggleton, Y. L. Ruan, and B. Luther-Davies, "Self-phase modulation-based integrated optical regeneration in chalcogenide waveguides," IEEE J. Sel. Top. Quantum Electron. **12**, 360-370 (2006).
13. M. D. Pelusi, V. G. Ta'eed, M. R. E. M. Lamont, S. , D. Y. Choi, B. Luther-Davies, and B. J. Eggleton, "Ultra-high Nonlinear As_2S_3 Planar Waveguide for 160 Gb/s Optical Time-Division Demultiplexing by Four-Wave Mixing," IEEE Photon. Technol. Lett. **19**, 1496-1498 (2007).
14. Y. L. Ruan, W. T. Li, R. Jarvis, N. Madsen, A. Rode, and B. Luther-Davies, "Fabrication and characterization of low loss rib chalcogenide waveguides made by dry etching," Opt. Express **12**, 5140-5145 (2004).
15. S. Madden, D.-Y. Choi, D. Bulla, A. Rode, B. Luther-Davies, V. G. Ta'eed, M. D. Pelusi, and B. J. Eggleton, "Long, low loss etched As2S3 chalcogenide waveguides for all-optical signal regeneration," Opt. Express **15**, 14414-14421 (2007).
16. M. Shokooh-Saremi, V. G. Ta'eed, N. J. Baker, I. C. M. Littler, D. J. Moss, B. J. Eggleton, Y. L. Ruan, and B. Luther-Davies, "High-performance Bragg gratings in chalcogenide rib waveguides written with a modified Sagnac interferometer," J. Opt. Soc. Am. B **23**, 1323-1331 (2006).
17. M. R. Lamont, C. M. d. Sterke, and B. J. Eggleton, "Dispersion engineering of highly nonlinear As_2S_3 waveguides for parametric gain and wavelength conversion," Opt. Express **15**, 9458-9463 (2007).

1. Introduction

While optical communication offers unprecedented data bandwidth, its efficient utilization requires the use of wavelength division multiplexing to overcome the speed limitations of current electronics. For wavelength routed networks, wavelength conversion is necessary to avoid the wavelength continuity constraint which otherwise restricts network efficiency [1]. All-optical wavelength conversion based on 3rd order nonlinear processes such as four-wave mixing (FWM), cross-gain modulation (XGM) or cross-phase modulation (XPM) can circumvent these limitations [1]. While FWM is efficient and data-format independent, it requires stringent phase-matching which cannot always be met [2]. XGM is associated with active media (e.g. semiconductor optical amplifiers) and care is required to overcome the long free-carrier lifetime which can produce pattern dependent effects, particularly at high data rates [3]. XPM based wavelength conversion, in contrast, does not require phase matching and can operate in passive media such as silica fiber [4], or highly nonlinear bismuth oxide [5] and chalcogenide glass [6, 7] fiber and waveguides.

Chalcogenide glasses have been known as an alternative platform for nonlinear signal processing for at least a decade [8]. These glasses possess the desirable combination of strong nonlinearity, intrinsically fast response time (not limited by free carriers as in silicon [9]), and low to moderate nonlinear absorption [10, 11]. These properties allow the development of a photonic chip that monolithically integrates several functions and that is capable of handling high data rate signals. Several of these functions have been demonstrated [12, 13], including wavelength conversion by XPM. Such devices have been restricted thus far by short nonlinear interaction lengths (≈5 cm) caused by fabrication induced propagation losses [14]. Recent advances [15] in planar fabrication have significantly reduced the propagation losses to around 0.05 dB/cm which allows the nonlinear interaction to occur efficiently over propagation distances greater than 50 cm, thereby reducing the optical power required for device operation.

In this paper we demonstrate broadband wavelength conversion at 40 Gb/s by XPM in a 22.5 cm long, low-loss As_2S_3 chalcogenide glass serpentine waveguide with a nonlinear coefficient ≈1700 $W^{-1}km^{-1}$ integrated onto a 7 cm chip. The longer interaction length reduced the required pulse power compared with previous experiments [7] allowed a four-fold increase in the signal data rate. While chalcogenide glasses exhibit strong normal dispersion in the near infrared wavelengths, this effect is minimized in the relatively short propagation length (compared to fiber) of the photonic chip device. Spectral measurements show that the device is effective over a span of 40 nm for an input signal centered at 1535 nm, while system measurements show just over 1 dB power penalty at a bit-error rate (BER) of 10^{-9}. Moreover, as the dispersion remains relatively constant, this device can be readily reconfigured to operate in any of the telecommunication bands (S, C or L bands).

#87558 - $15.00 USD Received 14 Sep 2007; revised 24 Oct 2007; accepted 26 Oct 2007; published 30 Oct 2007

2. Waveguide fabrication and characterization

Figure 1(a) shows the cross-section of a typical chalcogenide rib waveguide. The sample was fabricated [15] from As_2S_3 films thermally evaporated onto an oxidized silicon wafer, with the waveguide defined through photolithography and inductively-coupled plasma reactive-ion etching. The height of the resulting rib waveguides was 2.6 μm while the surrounding film was 1.7 μm. The waveguide was clad with a 15 μm thick film of UV cured inorganic polymer glass. The refractive index of the As_2S_3 film was 2.37 at 1550 nm, while that of the cladding polymer glass was 1.53. End facets were then prepared on the waveguide by hand cleaving the silicon substrate with a diamond scriber resulting in a ≈7 cm long chip. Following cleaving, the waveguide had a length of 22.5 cm consisting of 3 straight sections connected with two 180˚ bends of radii ≈3 mm. The mode-field area of the TE mode, calculated by c2V Olympios software, was found to be 7.1 μm^2 at 1550 nm while the group velocity dispersion was 435 ps^2/km – dominated by the material (≈466 ps^2/km).

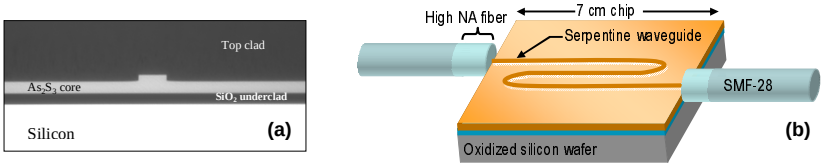

Fig. 1. (a). Optical micrograph of the As_2S_3 rib waveguide cross-section. (b) XPM takes place within the butt-coupled serpentine waveguide.

The nonlinear refractive index of As_2S_3 is $n_2 = 2.92^{-18}$ m^2/W [14], which yields a nonlinear coefficient approaching 1700 $W^{-1}km^{-1}$ at 1550 nm. The propagation loss at 1550 nm has been measured to be 0.05 ± 0.005 dB/cm for the TE mode, with 2.4 dB of PDL. The low propagation loss, 5× lower than previous waveguides [14] despite the additional complexity of the 3 mm bends [15], ensures the full length of the waveguide contributes towards nonlinear effects. Figure 1(b) shows the optical signals launched into the waveguide by butt-coupling single mode fiber (Corning SMF-28) pigtails with an intermediate length of higher numerical aperture fiber for improved mode-matching. Index matching fluid applied to the butt-couple minimized reflections, resulting in an insertion loss of 6.5 dB, of which only ≈1.1dB was due to propagation loss.

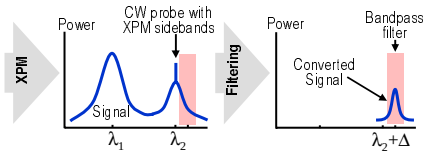

Fig. 2. CW probe at λ_2 experiences XPM from pulsed signal pump at λ_1 yielding XPM sidebands. Filtering of a single sideband results in conversion of the data signal to the new wavelength at $\lambda_2+\Delta$.

3. Device principle and setup

Figure 2 shows the device concept whereby XPM can be used as a simple and effective technique for achieving wavelength conversion of a return-to-zero data signal [4]. Pump pulses carrying data are directed though the nonlinear medium (serpentine chalcogenide glass waveguide) along with a continuous wave (CW) probe beam near the desired output wavelength. The pump pulses induce a transient chirp on the probe via XPM through the Kerr nonlinearity. This broadens the probe spectra generating sidebands, and when a single sideband is selected using an optical filter, the output wave at the converted wavelength is modulated in time similar to the pump pulse.

Figure 3 shows the experimental setup. The signal (pump) was generated from an optically filtered 40 GHz active mode-locked fiber laser (MLFL) producing ≈1.5 ps pulses centered at 1534.96 nm with a FWHM of 1.6 nm. An external electro-optic Mach-Zehnder (MZ)

#87558 - $15.00 USD Received 14 Sep 2007; revised 24 Oct 2007; accepted 26 Oct 2007; published 30 Oct 2007

modulator encoded a pseudorandom sequence of length 2^{31}-1 bits generated from a 40 Gb/s pattern generator. The pulse train was amplified using an low-noise EDFA and filtered to ≈0.62nm FWHM using two cascaded 1.3 nm band-pass filters (BPF), broadening the data pulses to 4.3 ps before being re-amplified. This amplified signal pump was combined, through a 70/30 coupler, with a CW probe, generated from an amplified external-cavity diode-laser, filtered with a 1.3nm BPF to remove out-of-band ASE. The polarization of both the pump and probe were controlled to allow alignment to the lower loss TE-mode of the waveguide and to maximise XPM. A sharp, 0.56nm BPF offset by ≈0.7-0.8 nm from the CW probe, selected a single XPM sideband which was then directed to the receiver which consisted of a low-noise amplifier, 1.3 nm BPF, variable optical attenuator (VOA) and 30 GHz photo-detector (PD). The MLFL, pattern generator and receiver were synchronized using an external 40 GHz RF clock.

The average signal pump power in the experiment was 23.8 dBm, while the CW probe power (at 1545 nm) was 19.7 dBm, resulting in a combined optical power of 25.2 dBm, or 326 mW, at the input facet of the As_2S_3 waveguide. This power value was not limited by the waveguide damage threshold (which remains unknown, though in excess of 400 mW), but rather by the amplifiers and coupler.

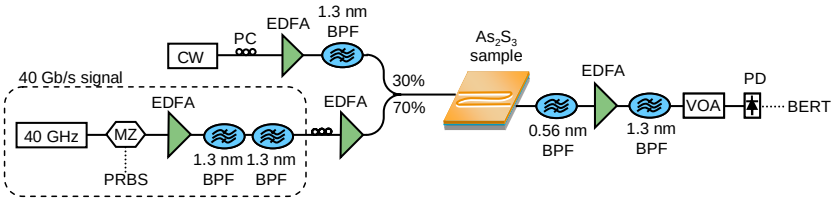

Fig. 3. Experimental setup for wavelength conversion by XPM.

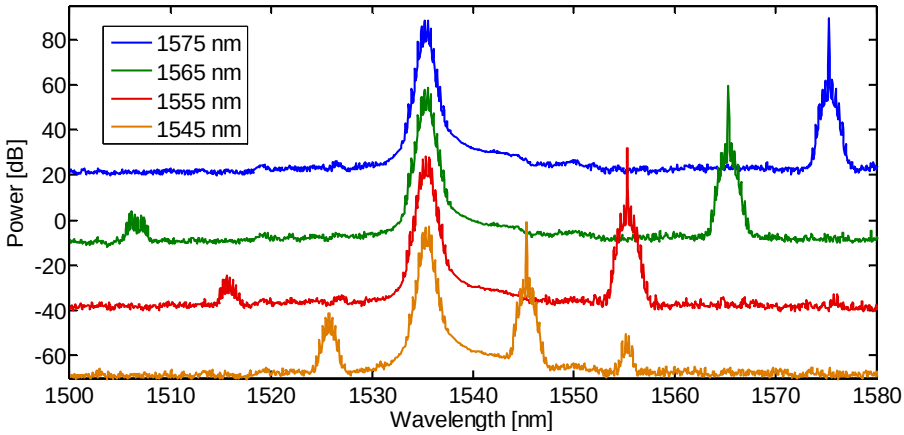

Fig. 4. Optical spectra from waveguide output for different CW probe wavelengths. (70 pm resolution bandwidth)

4. Experimental results

Figure 4 shows the optical spectra taken directly after the waveguide for the pump operating at 1535nm and the CW probe set to 4 different wavelengths (1545, 1555, 1565 and 1575 nm). The broad pedestals located at the base of the CW probe are the XPM induced sidebands, while the additional spectral components (e.g. at 1525, 1515 and 1505 nm, as well as the weak term at 1555 nm) are due to four-wave mixing (FWM) taking place between the pump and CW probe. FWM in these waveguides is relatively inefficient and wavelength dependent due to the effect of the strong normal dispersion within the waveguide. Nevertheless, such processes can be used for nonlinear optical signal processing, for example optical demultiplexing [13]. The XPM spectral sidebands are symmetric and independent of the CW

#87558 - $15.00 USD Received 14 Sep 2007; revised 24 Oct 2007; accepted 26 Oct 2007; published 30 Oct 2007

probe wavelength, indicating that pump-probe pulse walk-off, the limiting factor for spectral conversion range, is still small. The XPM sideband symmetry allows the short-wavelength sideband to be arbitrarily selected for wavelength conversion purposes.

Figure 5 compares the converted signal spectra data set for the CW probe spectrally located at 1545, 1555 and 1565 nm. Note the BPF used to select a single XPM sideband does not operate at the wavelength required to recover the signal for a CW probe of 1575 nm. For ease of comparison, the spectra in Fig. 5 are normalized to, and represented spectrally offset from, the residual CW probe component. While the residual CW probe is prominent, integration of the spectra data shows it corresponds to less than 5.8, 3.5 and 2.7% of the total converted signal power for each of the respective data sets. The ASE hump at frequencies >200 GHz corresponds to less than 0.5% of the total power in the signal in all three data sets.

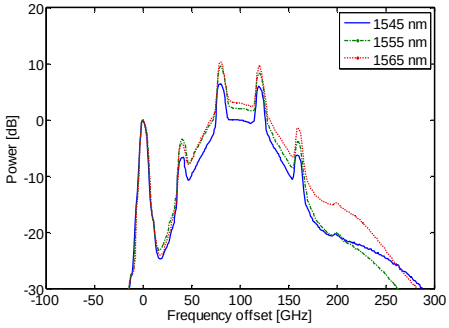

Fig. 5. Converted spectra, normalized and spectrally relative to residual CW probe. (70 pm resolution bandwidth)

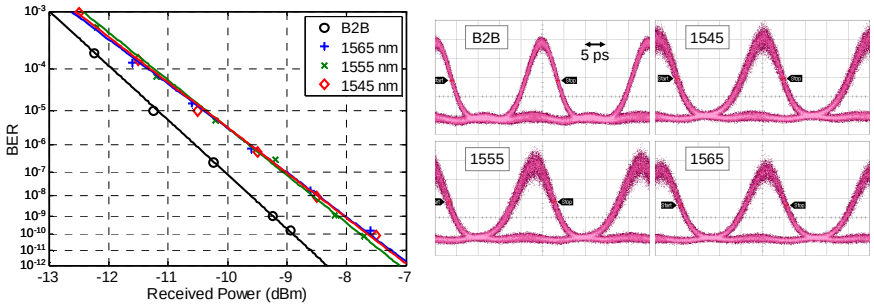

Fig. 6. Left: Data eye diagram (65GHz optical bandwidth detector) for 40 Gb/s back-to-back input (B2B) and wavelength converted signals. Right: BER versus received optical power for back-to-back (B2B) and converted signals.

Figure 6 shows clean, open data eye for the converted signals with some additional noise present in the marks – suggesting a low system penalty can be expected. From autocorrelation measurements of the converted output, the deconvolved pulse duration, assuming Gaussian profile, is 6.3 ps.

Figure 7 gives the BER as a function of the received optical power, showing no floor or wavelength dependence, as anticipated from the pulse spectra and eye-diagrams. The power penalty for a BER = 10^{-9} was 1.2, 1.1 and 1.2 dB for the three converted signals with respect to the 40 Gb/s back-to-back (B2B) signal received at the VOA. From the spectral data in Fig. 5 as well as observation of low signal distortion in Fig. 6, the source of this penalty is likely due to in-band ASE contributing to the noisy marks as well as a small power offset due to the residual CW probe.

5. Discussion

In our earlier report [7] of XPM based wavelength conversion in As_2S_3 waveguides, device performance was limited by the short propagation length (5 cm) and conservative estimates on

#87558 - $15.00 USD Received 14 Sep 2007; revised 24 Oct 2007; accepted 26 Oct 2007; published 30 Oct 2007

the damage threshold, resulting in the use of low duty cycle signals (2.1 ps pulses at 10 Gb/s) to obtain the necessary peak optical power. In this paper, the combination of longer, lower-loss waveguides and *higher* optical power have enabled a four-fold increase in the data rate, as well as an eight-fold increase in the signal duty cycle (4.3 ps pulses at 40 Gb/s).

In the previous experiments an additional fiber Bragg grating notch filter was required in order to remove residual CW probe. This was circumvented in this paper through use of a sharp output filter (0.56 nm) resulting in 6.3 ps duration output pulses – optimum for a 25% duty cycle 40 Gb/s, return-to-zero signal. We anticipate that a reduction of the effective core area of the waveguide or optimization of the nonlinear refractive index will enable operation of the device with the same 25% duty cycle at the input.

While the power penalty in the system measurements was only just over 1 dB, a comment is called for on conversion efficiency and performance limits. As this device uses phase modulation of a co-propagating probe beam, measuring conversion efficiency relative to the input signal is meaningless (probe power can be changed arbitrarily). Even efficiency characterized as a ratio of output signal to input probe power is limited by the use of amplification between the dual stage filters. In this demonstration, performance was noise limited, as evinced by the converted spectra seen in Fig. 5. Increasing the nonlinear phase shift (via glass nonlinearity, waveguide cross-section and interaction length or power) and associated XPM spectral broadening will improve device performance in terms of the optical signal to noise ratio of the converted signal, as would directly increasing the pump or probe power. This can potentially also allow the side-band extraction setup at the waveguide output to be significantly simplified, for example by integrating the filtering through photosensitive inscribed Bragg gratings for added monolithic functionality [16].

While long waveguides were used, the group velocity difference between the pump and phase modulated CW probe was small allowing broadband wavelength conversion. For a 40 nm wavelength offset, the walk-off length [2] is calculated to be ≈19 cm – just short of the waveguide length. Reducing the waveguide transverse dimensions will yield changes in the group velocity dispersion due to waveguide effects which can be used to shift the zero-dispersion wavelength towards and even into the telecommunications band [17]. This will have the result of added conversion bandwidth, but also access to efficient four-wave mixing processes.

6. Conclusion

We demonstrate broadband wavelength conversion of a 40 Gb/s signal by cross-phase modulation within a 22.5 cm long, As_2S_3 rib waveguide. System measurements show power penalties just in excess of 1 dB at a BER of 10^{-9} over a span of 30 nm. The low-loss of these waveguides ensures the full propagation length contributes towards the nonlinear process, allowing a significant reduction in the required peak operating power. This in turn has allowed a four-fold increase in the signal data rate compared to previous demonstrations in both fiber and planar waveguide formats. While the group velocity dispersion value of As_2S_3 chalcogenide glass is large, the short propagation length (relative to fiber) ensures that this effect is minimized resulting in strong cross-phase modulation sidebands for wavelength offsets as great as 40 nm. Analysis indicates that enhancement of the nonlinearity of the chalcogenide glass composition or reductions in waveguide transverse dimensions will lead to significant performance gains, as well as to access to efficient four-wave mixing processes. Lastly, potential exists for integrating the filters via photosensitive inscribed Bragg gratings.

Acknowledgment

The support of the Australian Research Council through its Centres of Excellence and Federation Fellow programs is gratefully acknowledged.

#87558 - $15.00 USD Received 14 Sep 2007; revised 24 Oct 2007; accepted 26 Oct 2007; published 30 Oct 2007